HAL
open science

Kinetic modeling of the sesamin conversion into asarinin in the presence of citric acid loading on Hβ

Qiong Yu, Xiao-Shuang Cai, Sébastien Leveneur, Xue-De Wang, Hua-Min Liu, Chen-Xia Zhang, Yu-Xiang Ma

To cite this version:

Qiong Yu, Xiao-Shuang Cai, Sébastien Leveneur, Xue-De Wang, Hua-Min Liu, et al.. Kinetic modeling of the sesamin conversion into asarinin in the presence of citric acid loading on Hβ. Frontiers in Nutrition, In press, 10.3389/fnut.2022.983843 . hal-03749209

HAL Id: hal-03749209

https://normandie-univ.hal.science/hal-03749209

Submitted on 10 Aug 2022

HAL is a multi-disciplinary open access archive for the deposit and dissemination of scientific research documents, whether they are published or not. The documents may come from teaching and research institutions in France or abroad, or from public or private research centers.

L'archive ouverte pluridisciplinaire **HAL**, est destinée au dépôt et à la diffusion de documents scientifiques de niveau recherche, publiés ou non, émanant des établissements d'enseignement et de recherche français ou étrangers, des laboratoires publics ou privés.

frontiers | Frontiers in Nutrition

TYPE Original Research
PUBLISHED 10 August 2022
DOI 10.3389/fnut.2022.983843

Check for updates

OPEN ACCESS

EDITED BY
Massimo Lucarini,
Council for Agricultural Research and Economics, Italy

REVIEWED BY
Michael Murkovic,
Graz University of Technology, Austria
Shuai Chen,
Wuhan University, China

*CORRESPONDENCE
Xue-de Wang
13903865584@126.com

SPECIALTY SECTION
This article was submitted to Nutrition and Food Science Technology,
a section of the journal Frontiers in Nutrition

RECEIVED 01 July 2022
ACCEPTED 25 July 2022
PUBLISHED 10 August 2022

CITATION
Yu Q, Cai X-s, Leveneur S, Wang X-d, Liu H-m, Zhang C-x and Ma Y-x (2022) Kinetic modeling of the sesamin conversion into asarinin
in the presence of citric acid loading on Hβ.
Front. Nutr. 9:983843.
doi: 10.3389/fnut.2022.983843

COPYRIGHT
© 2022 Yu, Cai, Leveneur, Wang, Liu, Zhang and Ma. This is an open-access article distributed under the terms of the Creative Commons Attribution License (CC BY). The use, distribution or reproduction in other forums is permitted, provided the original author(s) and the copyright owner(s) are credited and that the original publication in this journal is cited, in accordance with accepted academic practice. No use, distribution or reproduction is permitted which does not comply with these terms.

Kinetic modeling of the sesamin conversion into asarinin in the presence of citric acid loading on Hβ

Qiong Yu[1], Xiao-shuang Cai[1], Sébastien Leveneur[2], Xue-de Wang[1]*, Hua-min Liu[1], Chen-xia Zhang[1] and Yu-xiang Ma[1]

[1]College of Food Science and Engineering & Institute of Special Oilseed Processing and Technology, Henan University of Technology, Zhengzhou, China, [2]INSA Rouen, UNIROUEN, LSPC, UR4704, Normandie Université, Rouen, France

In the present work, effects of reaction temperature, reactant concentration, catalyst loading, and rotation speed on the kinetics of sesamin conversion in a sesame oil system were studied by using citric acid loading on Hβ zeolite (CA/Hβ) as a catalyst. A kinetic model was built for sesamin conversion. The kinetic model fits correctly the experimental concentration of sesamin and asarinin ($R^2_{Sesamin}$ = 0.93 and $R^2_{Asarinin}$ = 0.97). The sesamin conversion is an endothermic reaction ($\Delta H_{r\ \mathrm{Iso}}$ = 34.578 kJ/mol). The CA/Hβ catalyst could be easily regenerated by calcination, and there was no obvious loss of catalytic activity when reused. Knowledge of the sesamin conversion is of great significance for guiding production and improving the value and nutrition of sesame oil. In a word, this study lays the foundation for the scale-up of the production of asarinin from sesame oil using CA/Hβ as the catalyst.

KEYWORDS

sesamin, asarinin, catalyst, sesame oil, kinetic modeling

Introduction

Lignans have been shown to possess a variety of physiological activities (1–3). Asarinin is a furofuran lignan. According to reports, compared to sesamin, asarinin has strong physiological activities such as anti-cancer, anti-proliferative (4), antioxidative (5), and antibacterial. It was reported that asarinin was yielded when sesamin was oxidized by potassium permanganate under acidic conditions. It was found that at the same concentration, the inhibition rate of asarinin on DPPH free radical reached 43.3%, while the inhibition rate of sesamin is 27.2% (5). Kim et al. (6) reported that asarinin and sesamin showed cytotoxicity with IC_{50} values of 67.25 and 98.57 μM, respectively, in MCF-7 cells. It was found that asarinin can increase the activity and gene expression of fatty acid oxidation enzymes of rats more strongly than sesamin (3). Asarinin has

10.3389/fnut.2022.983843

the potential to be clinically applied to induce cancer cell death and inhibit metastasis because of its antiangiogenic properties (7).

Asarinin is a geometrical isomer of sesamin generated under certain conditions of temperature and acidity (8). It is formed from sesamin during refining processes (i.e., acid clay bleaching and deodorization at high temperature) (9, 10). Compared with homogeneous catalysts (e.g., hydrochloric acid and sulfuric acid), heterogeneous catalysts such as phosphotungstic acid (11), acid cation exchange resin (12), acid clay (13), and Hβ zeolite (14) have the advantages of easier separation and recycling. Owing to its surface acidity and special porous structure, zeolite beta is a commonly used solid acid catalyst (SACs). Zeolite beta is widely applied in refining and in the chemical industry for various reactions such as isomerization, esterification, and alkylation (15–17). The maximum conversion rates for esterification of oleic acid and transesterification of soybean oil by the use of modified Hβ zeolite were 86% and 95%, respectively. The catalyst can be recycled up to four times without any loss during the conversion process (18).

The mechanism of sesamin conversion in a sesame oil system is illustrated in **Figure 1** (8, 10). In a sesame oil system, CA/Hβ attacks the O atom on the tetrahydrofuran ring of sesamin and absorbs it into the active center of CA/Hβ. An unstable intermediate transition state forms in this process. Asarinin is produced through the desorption of the intermediate transition state; at the same time, CA/Hβ is regenerated.

For practical application, it is vital to be able to evaluate and predict the changes of sesame lignans under process conditions. Consequently, a reliable kinetic model is often needed. While there have been studies of the kinetics of the lipid peroxidation (19, 20) of vegetable oils and of biodiesel fuel (21) production from vegetable oils, the kinetics of sesamin conversion in a sesame oil system have not been studies. One research group noticed that the kinetics of sesamin conversion is of first-order in the ethanol-sesamin system by using hydrochloric acid as a catalyst (22). To the best of our knowledge, no kinetic models have been developed for the sesamin conversion in sesame oil system. The SACs studied here, which was used in our previous work, showed good catalytic performance (14, 23). In this study, the kinetics of the sesamin conversion with CA/Hβ in cold-pressed sesame oil (CSO) was investigated. Influences of reaction parameters including temperature, reactant concentration, catalyst loading, and rotation speed on the kinetics of sesamin conversion were evaluated. Kinetic modeling was developed to estimate the rate constants and activation energy of sesamin conversion with the catalyst CA/Hβ under these reaction conditions. This study provides a theoretical foundation for controlling conditions promoting the sesamin conversion, and the mass production of high-quality sesame oils rich in asarinin.

Experimental section

Materials and chemicals

Chromatographic-grade methanol was obtained from VBS Biologic INC, United States. Hydrogen type of zeolite beta with a Si/Al ratio of 25 (Hβ) was purchased from the Nankai University catalyst plant, Tianjin, China. Sesamin was obtained from Macklin Biochemical Co., Ltd., Shanghai, China. Asarinin was purchased from Purechem-standard Co., Ltd., Chengdu, China. Citric acid (CA) was obtained from Shanghai Yuanye Biotechnology Co., Ltd., Shanghai, China. The standard substances were stored at 4°C in darkness. CSO was made in a hydraulic press (Bafang Ltd., model XL-600, Suzhou, China) in our laboratory.

Preparation of sesame oil samples

Considering the content and the solubility of sesamin in sesame oil, a certain amount of sesamin (30 and 60 mg) was added to 70 g sesame oil, and then the mixture was treated with ultrasound for 30 min, subsequently, the mixture was placed in a thermostatic magnetic water bath stirred for 4 h at 37°C (24). Sesamin and asarinin contents in all sesame oil samples were analyzed using HPLC-UV (high-performance liquid chromatography combined with ultraviolet detector) methods based on the pervious literature (25, 26). The sesamin conversion (%) was calculated using the following equation:

$$\textit{sesamin conversion \%} = \left(1 - \frac{C_A}{C_{A0}}\right) \times 100$$

where, C_{A0} (mg/100 g) is the initial concentration of sesamin in the sesame oil, and C_A (mg/100 g) is the sesamin concentration at a particular time in the reaction process.

Preparation of catalyst

Citric acid loading on Hβ was prepared on the basis of the reported literature (17, 23, 27). Briefly, a 20 g sample of Hβ was added to 200 ml of critic acid aqueous solution, and the resulting suspension was stirred at room temperature for 16 h. And then washed, dried and calcined. The catalyst has been proven to promote the conversion of sesamin into asarinin and shows well activity (14).

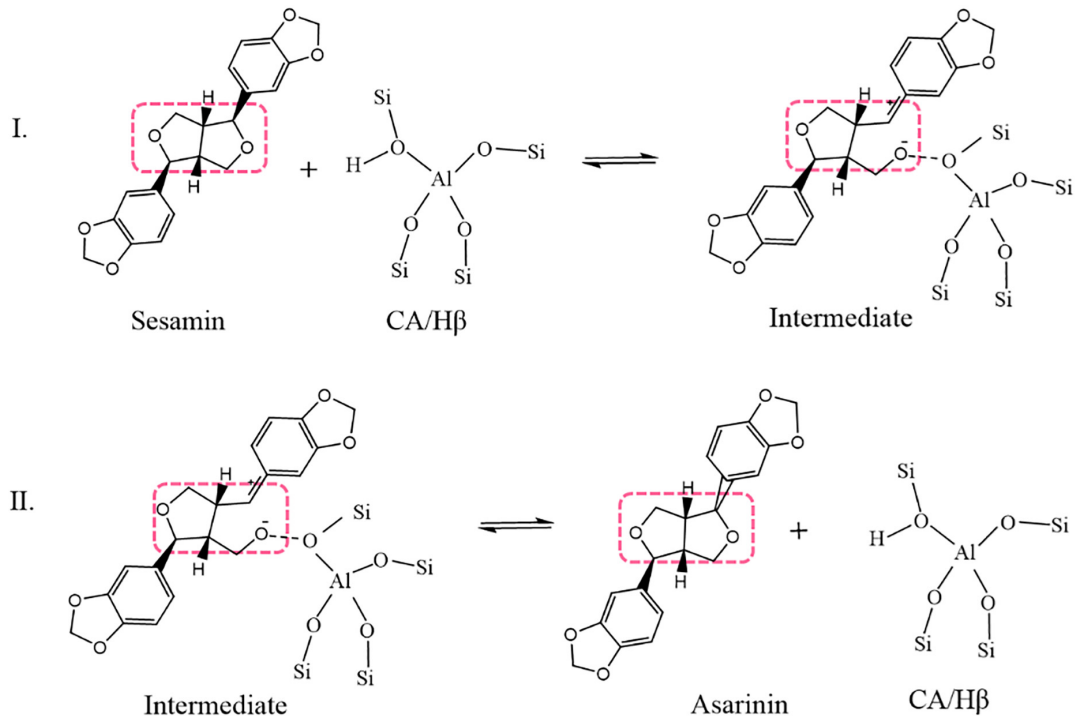

FIGURE 1
Simplified mechanism of sesamin conversion in sesame oil (dotted boxes enclose tetrahydrofuran rings).

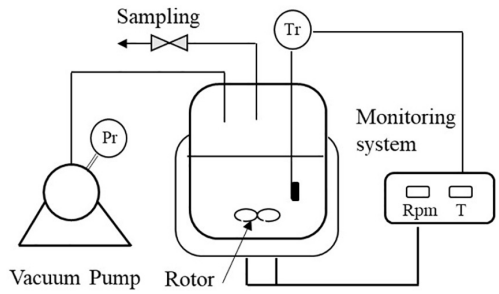

FIGURE 2
Schematic of reaction setup.

TABLE 1 Experimental matrix for the sesamin conversion.

Run	Initial reactant C_A mmol/L	T °C	Catalyst loading wt.%	Rotation speed rpm
1	21.47	80	1.6	300
2	23.83	80	1.6	300
3	22.91	80	1.6	300
4	21.47	70	1.6	300
5	21.47	90	1.6	300
6	21.47	80	1.0	300
7	21.47	80	3.0	300
8	21.47	80	1.6	200
9	21.47	80	1.6	400

Apparatus and experimental procedures

The reaction apparatus is shown in Figure 2. Experiments were performed in a 250 ml glass-jacket reactor equipped with a magnetic stirrer, vacuum pump and temperature control system.

Kinetic study of sesamin conversion

In total, 50 g of CSO was added to the 250 ml glass-jacket reactor at a certain stirring speed (see Table 1). When the oil temperature reached the set temperature, a specific amount of catalyst was added into the reactor vessel. Agitation was started. 2.0 ml sesame oil samples were collected at specific time points. The sesame oil sample was immediately placed in an ice water bath to quench the reaction and then centrifuged. The sesame oil samples were stored at −20°C for analysis within 2 days.

Table 1 displays the experimental matrix for each run with the detailed reaction conditions. The parameters affecting sesamin conversion of sesame oil were reaction temperature (70–90°C), initial concentration of sesamin (21.47–23.83 mmol/L), catalyst loading (1.0–3.0%) and rotation

speed (200–400 rpm). These parameters were selected according to the results of previous tests (14). C_A (mg/100 g) and C_B (mg/100 g) represent the concentrations of sesamin and asarinin, respectively, in the oil samples during the whole reaction process. At the beginning of all kinetic experiments, there was no asarinin; consequently, the concentration of asarinin was zero at time zero.

Recycling of the catalyst

After execution of the conversion reaction, the reaction mixture was centrifuged at 4,500 rpm for 20 min. The CA/Hβ catalyst was separated, washed with n-hexane and dried in an oven at 60°C, and then, the recycled catalyst was calcined in a muffle furnace (500°C) for 4 h. The reused catalyst was characterized by N_2 adsorption and desorption isotherm analysis (Micromeritics, 3-Flex, United States). The surface areas of catalysts were calculated by BET method using adsorption data (28).

Modeling

Athena Visual Studio software was used for parameter estimation (29, 30). During the kinetic modeling stage, the concentrations of sesamin and asarinin were used as observables. DDAPLUS solver, included in Athena Visual Studio, integrates ordinary differential equations (ODEs) (10, 11). This solver is a modified Newton algorithm used in conjunction with a fixed leading coefficient backward difference formula for the approximation of first-order derivatives (31). In this study, the modeling dealt with a multi-response parameter estimation. The GREGPLUS subroutine package included in Athena Visual Studio was applied to minimize the objective function $S(\theta)$, and calculate the maximum posterior probability density of the various estimated parameters and the values of the posterior distribution of the tested models (30). The objective function was defined as

$$S(\theta) = (n + m + 1) \cdot ln\,|\upsilon(\theta)| \quad (1)$$

where, m is the number of responses, n is the number of events in response and $|\upsilon(\theta)|$ is the determinant of the covariance matrix of the responses. Each element of this matrix is denoted as:

$$\upsilon_{ij}(\theta) = \sum_{u=1}^{n} [Y_{iu} - Y_{iu}(\theta)] \cdot \left[Y_{ju} - Y_{ju}(\theta)\right] \quad (2)$$

with Y_{iu} the experimental concentration and $Y_{iu}(\theta)$ the estimated value for the response i, and event u; $Y_{ju}$is the experimental concentration, *via* the estimated parameters θ, $Y_{ju}(\theta)$ is the estimated value for the response j, and event u. The precision of the estimated parameters was evaluated by the 95% marginal highest posterior density (HPD). The 95% HPD was calculated by the GREGPLUS package.

Statistical analysis

All measurements were carried out in triplicate and the data were expressed as mean values.

Results and discussion

Kinetic study

In this section, the effect of reaction temperature (70–90°C), catalyst loading (1.0–3.0%), rotation speed (200–400 rpm) and initial concentrations of reactant (21.47, 22.91, and 23.38 mmol/L) on the kinetics of sesamin conversion were investigated. The sesamin conversion was selected as a response value, and its kinetic curves are plotted in **Figures 3A–D**.

Effect of rotation speed

Three levels of rotation speeds (200, 300, and 400 rpm) were applied to reveal the influence of external mass transfer on the reaction kinetics. Experiments were performed under the following conditions: sesame oil temperature, 80°C, catalyst (CA/Hβ) loading, 1.6% and initial concentration of reactant, 21.47 mmol/L (**Figure 3A**). As the reaction proceed, the conversion of sesamin became lower. Experiments conducted at 200, 300, or 400 rpm displayed similar kinetics. There was no significant difference in sesamin conversion at 200 and 300 rpm. The conversion of sesamin decreased slightly when the rotation speed was 400 rpm. The stirring speed was found to have minor effects on the kinetics of sesamin conversion. The reason might be related to contact between the reactants and the active surface of the catalyst. This phenomenon is similar to the results reported previously (32).

Effect of reaction temperature

The effect of reaction temperature (70, 80, and 90°C) on the sesamin conversion in sesame oil was investigated. The reaction parameters were as follows: catalyst (CA/Hβ) loading, 1.6%; rotation speed, 300 rpm; initial concentration of reactant, 21.47 mmol/L. As illustrated in **Figure 3B**, as the reaction temperature increased from 70 to 90°C, the conversion rate of sesamin also significantly increased. This phenomenon has been observed in previous studies when inorganic acid was used as catalyst for the sesamin conversion in an ethanol system (22). In general, high

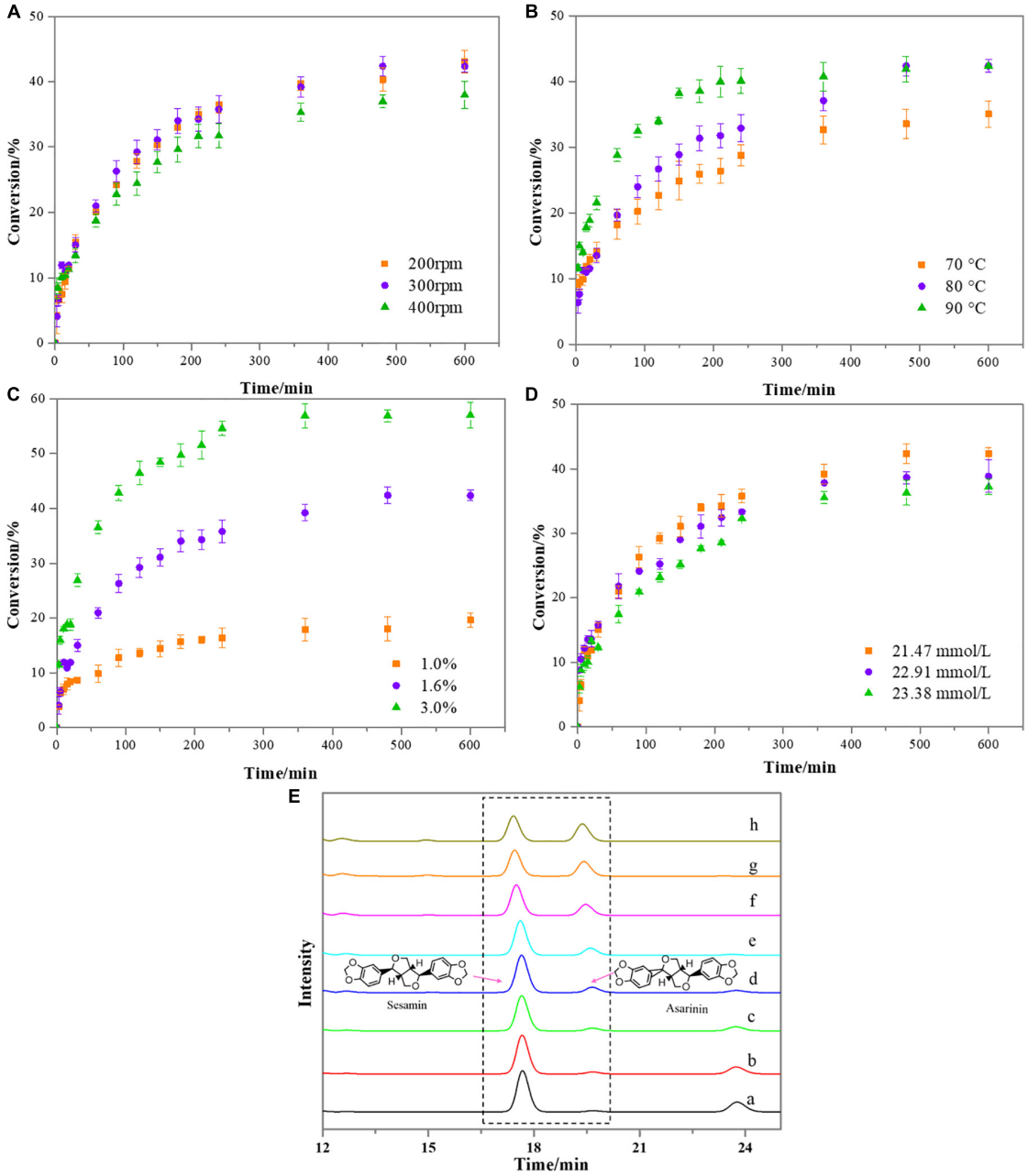

FIGURE 3
Effect of reaction conditions on the kinetics of the sesamin conversion under the following conditions: **(A)** catalyst loading, 1.6%; sesame oil temperature, 80°C; reactant concentration, 21.47 mmol/L; **(B)** catalyst loading, 1.6%; rotation speed, 300 rpm; reactant concentration, 21.47 mmol/L; **(C)** sesame oil temperature, 80°C; rotation speed, 300 rpm; reactant concentration, 21.47 mmol/L. **(D)** Catalyst loading, 1.6%; sesame oil temperature, 80°C; rotation speed, 300 rpm. Bars represent standard deviation (n = 3). **(E)** Variation in absorbance intensity of sesamin and asarinin in sesame oil samples at different reaction times under the following conditions: catalyst loading, 3.0%; sesame oil temperature, 80°C; rotation speed, 300 rpm; reactant concentration, 21.47 mmol/L (a, 3 min; b, 5 min; c, 10 min; d, 20 min; e, 30 min; f, 1.0 h; g, 2.0 h; h, 3.0 h).

temperature reduces the viscosity of the oil and thus increases the mass transfer rate (33, 34). At the reaction time of 240 min, the sesamin conversion increased with temperature, as follows: 23.72% (70°C) < 35.78% (80°C) < 40.09% (90°C).

Effect of catalyst loading

The influence of catalyst loading on sesamin conversion in sesame oil samples is illustrated in Figure 3C. The catalyst loading at three levels (1.0, 1.6, and 3.0% of

sesame oil) were studied, using the following reaction conditions: sesame oil temperature, 80°C; initial concentration of reactant, 21.47 mmol/L; rotation speed, 300 rpm. From the data shown in **Figure 3C**, as catalyst loading increased, the conversion rate of sesamin increased, indicating that there was no mass-transfer limitation in this test. The reason might be that the more active sites provided by the catalyst, the faster the conversion rate (35). At the reaction time of 240 min, the sesamin conversion was 16.38% at 1.0% catalyst loading, 35.78% at 1.6% catalyst loading, and 54.78% at 3.0% catalyst loading.

Effect of initial concentration of reactant

Figure 3D shows the effect of initial reactant concentration on the sesamin conversion under the following conditions: reaction temperature, 80°C; rotation speed, 300 rpm; catalyst loading, 1.6%. The results showed that the kinetic rate decreased slightly with the increase of the initial concentration of reactant. At the reaction time of 240 min, the sesamin conversion reached 35.78% at the reactant concentration of 21.47 mmol/L. The sesamin conversion was 33.34 and 32.27% at the reactant concentrations of 22.91 and 23.38 mmol/L, respectively. There was no significant difference among different initial concentrations of reactant. Sesamin was found to have poor solubility when it was added back to sesame oil (26). In this test, it was assumed that sesamin was dissolved in the sesame oil when no crystallization of sesamin in the sesame oil was observed with the naked eye. As for the phenomenon that the conversion rate was relatively lower when the concentration of reactant was slightly higher, it is possible that there were crystals blocking the active sites on the catalyst surface (35).

Variation of peak areas in liquid chromatograms

In order to monitor the evolution of sesamin and asarinin, samples withdrawn at different times during the reaction were analyzed by HPLC-UV. The peak at 17 min corresponds to the substance sesamin, and the peak at 19 min is asarinin. It was observed intuitively from **Figure 3E** that the peak area of sesamin was decreased gradually and asarinin increased with the reaction time going on. This was interpreted to mean that, as the reaction proceeded, sesamin was partially converted to asarinin. These results are consistent with previous studies (8, 9).

Reusability and characterization of citric acid loaded on Hβ

Easy recycle and reusability are the main advantage of heterogenous catalysts (36). The reusability of the CA/Hβ catalyst was evaluated by the sesamin conversion reaction at a temperature of 80°C and rotation speed of 300 rpm, with a catalyst loading of 3.0%. As shown in **Figure 4A**, the CA/Hβ catalyst exhibited good recyclability in the sesamin conversion, the sesamin conversion decreased insignificantly, from 59.21 to 57.49% at 240 min.

The textural characteristics of catalyst was assessed by N_2 adsorption and desorption isotherm analysis (**Figures 4B–D**) (28, 37). According to the classification of international union of pure and applied chemistry (IUPAC), the isotherm of the catalysts displayed a combination of type I and type IV isotherms. It is clear that, at lower relative pressures (P/P_0 = 0.0–0.1), the catalysts showed isotherm type I, which corresponds to microporous material. A hysteresis loop was observed at the upper section of isotherm over the relative pressure range from 0.7 to 1.0, indicating that there were mesopores in the solid. This is further demonstrated in the BET analysis results in **Table 2**.

The structural properties including surface area, pore volume and pore size of reused catalysts were summarized in **Table 2**) (38). After the catalyst was calcined at 500°C for 4 h, the specific surface area, pore size and pore volume renew to that of the fresh catalyst, and the seamin conversion was almost the same as that of the fresh catalyst (**Table 2** and **Figure 4A**). It shows that calcination could remove the most of the organic substance adsorbed on the catalyst. A slight descend of pore size was observed in each recycle of the catalyst, which was consistent with the reduction of sesamin conversion. It may be that the effect of separation and n-hexane washing on the catalyst, and part of the active site of the catalyst is blocked by organic substance (35). In brief, these results revealed that the catalytic activity of the regenerated catalyst was almost the same as that of the fresh catalyst used for the first time (1st). The catalytic of catalyst could be reversed easily by calcination.

Kinetics

According to the published literature (8, 9, 22), the sesamin conversion is reversible under certain conditions. The overall reaction can be represented as follows:

$$A \overset{\text{catalyst}}{\rightleftharpoons} B \tag{3}$$

Based on the mechanism in **Figure 1**, the conversion reaction can be described in three steps. The first step is the opening of sesamin's furan ring with catalyst, forming

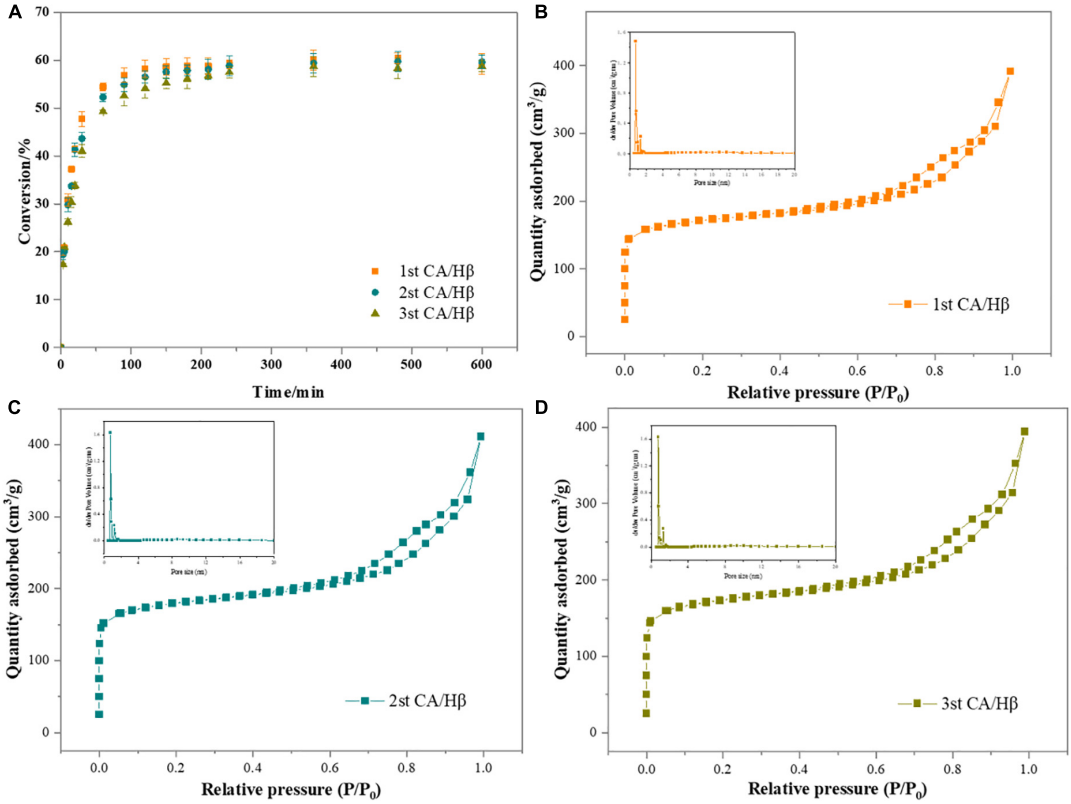

FIGURE 4
(A) The sesamin conversion with recycled catalyst. Reaction conditions: catalyst loading, 3.0%; sesame oil temperature, 80°C; rotation speed, 300 rpm; **(B–D)** N_2 adsorption and desorption isotherms of recycled catalyst.

TABLE 2 Surface properties of catalysts.

	BET surface area/m²/g	External surface area m²/g	Pore size (nm)	Pore volume (cm³/g)	Micropore volume (cm³/g)	Mesopore volume (cm³/g)
1st CA/Hβ	552.48	140.79	4.39	0.61	0.20	0.40
2st CA/Hβ	579.38	147.27	4.39	0.64	0.21	0.42
3st CA/Hβ	560.62	143.46	4.35	0.61	0.20	0.41

intermediate I_1. The second step is the intermediate I_1 turning into an intermediate of asarinin and catalyst; the third step is the desorption of the intermediate of asarinin and catalyst to release asarinin and catalyst.

$$\mathrm{A} \underset{k_{-1}}{\overset{K_1}{\rightleftharpoons}} \mathrm{I}_1 \tag{4}$$

$$\mathrm{I}_1 \underset{k_{-2}}{\overset{K_2}{\rightleftharpoons}} \mathrm{B}{-}^{*} \tag{5}$$

$$\mathrm{B}{-}^{*} \overset{K_3}{\rightleftharpoons} \mathrm{B}{+}^{*} \tag{6}$$

where A is sesamin, B is asarinin, K_1, K_2, and K_3 are the equilibrium constants; $[I_1]$ is the concentrations of intermediate I_2, mol/L; $[*]$ is the concentration of the catalytic active sites at time t, mol/L, $[\mathrm{B}-*]$ represents the product of asarinin coupling with the active sites of catalyst at time t, mol/L. Assuming that the second step is the rate-determining step, the kinetics of the conversion reaction can be expressed as:

$$R_{\mathrm{Iso}} = R_2 = (k_2\,[I_1] - k_{-2}\,[\mathrm{B}]\,)w_{\mathrm{cat}} \tag{7}$$

When the quasi-equilibrium approximation is applied to the intermediates,

$$K_1 = \frac{[I_1]}{[\mathrm{A}]\,[*]}, K_2 = \frac{[\mathrm{B}-*]}{[I_1]}\ and\ K_3 = \frac{[\mathrm{B}]\,[*]}{[\mathrm{B}-*]} \tag{8}$$

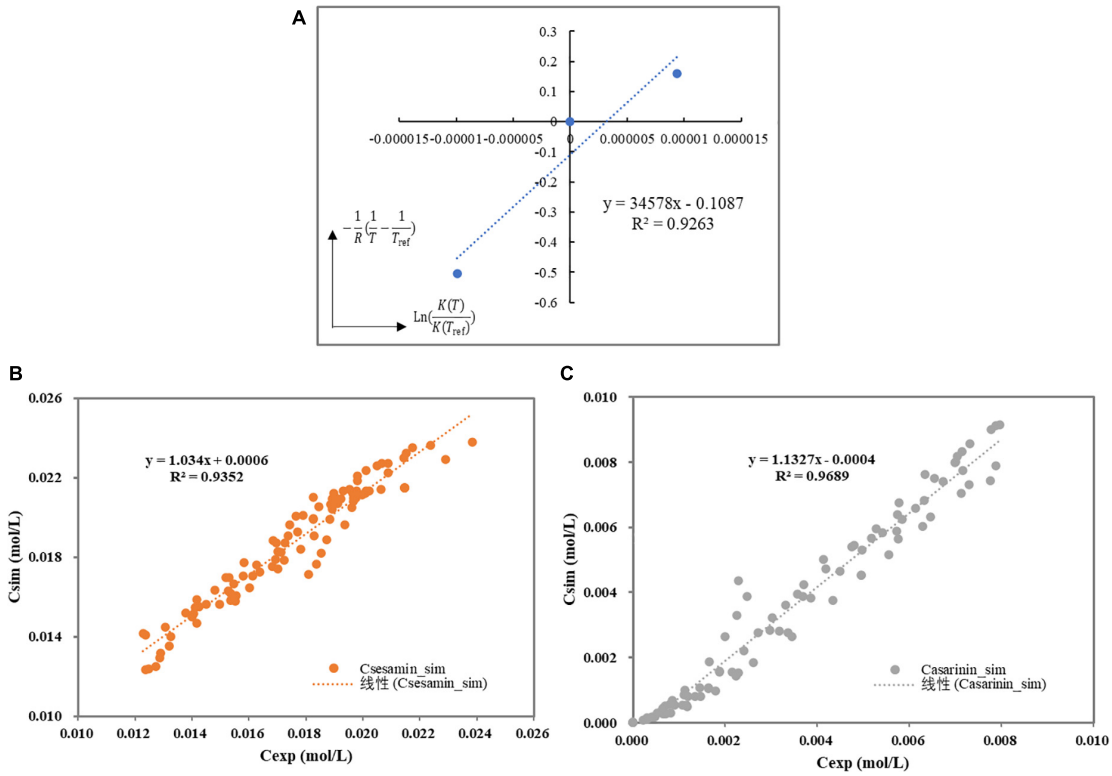

FIGURE 5
(A) Van't Hoff curve for Henry's constants. **(B)** Parity plot of experimental versus simulation of the sesamin concentration. **(C)** Parity plot of experimental versus simulation of the asarinin concentration.

TABLE 3 Estimated and statistical data at T_{ref} = 353.15K for sesamin conversion.

	Estimated value	95% marginal HPD intervals	HPD in %
$\mathrm{Ln}k_{Iso}(T_{ref})$ (L mol^{-1} s^{-1})	9.74E+00	6.97E−02	0.72
$Ea/(RT_{ref})$	2.14E+01	3.91E+00	18.23
K_1	4029.99	Indeterminate	–
K_{Iso} (T_{ref})	0.536	–	–
H_{Iso} (J mol^{-1})	34578	–	–

The concentration of intermediate I_1 can be expressed as

$$[I_1] = K_1\,[\mathrm{A}]\,[*] \tag{9}$$

By combining Eqs 6, 7, the conversion kinetics become

$$R_{\mathrm{Iso}} = (k_2 K_1\,[\mathrm{A}]\,[*] - k_{-2}\,[\mathrm{B}])w_{\mathrm{cat}} \tag{10}$$

where w_{Cat} is the catalyst loading in g/L.

Mass balance

Experiments were carried out in a vacuum. We assumed $K_1 = K_2$, and that the mass balance applied to the surface

TABLE 4 Correlation matrix of kinetics modeling.

	$\mathrm{Ln}k_{Iso}(T_{ref})$	$Ea/R(T_{ref})$	K_1
$\mathrm{Ln}k_{Iso}(T_{ref})$	1		
Ea/RT_{ref}	−0.157	1	
K_1	0	0	0

species leads to

$$[*]_0 = [*] + [I_1] + [\mathrm{B}{-}*] \tag{11}$$

where, $[*]_0$ is the total concentration of the catalytic active sites, mol/L. The concentration of active sites at time t is

$$[*] = \frac{[*]_0}{1 + K_1\,[\mathrm{A}] + K_2[\mathrm{B}]} \tag{12}$$

When the following notations are introduced: $k_{Iso} = K_1 k_2$, $K_{Iso} = k_2/k_{-2}$, Eq. 6 becomes

$$R_{\mathrm{Iso}} = k_{\mathrm{Iso}} \times \frac{w_{\mathrm{cat}}}{1 + K_1\,[A] + K_2[B]} \times \left([A] - \frac{1}{K_{\mathrm{Iso}}}\,[\mathrm{B}]\right) \tag{13}$$

All the associated parameters were estimated during the kinetic modeling stage (39, 40). The following ODEs describe

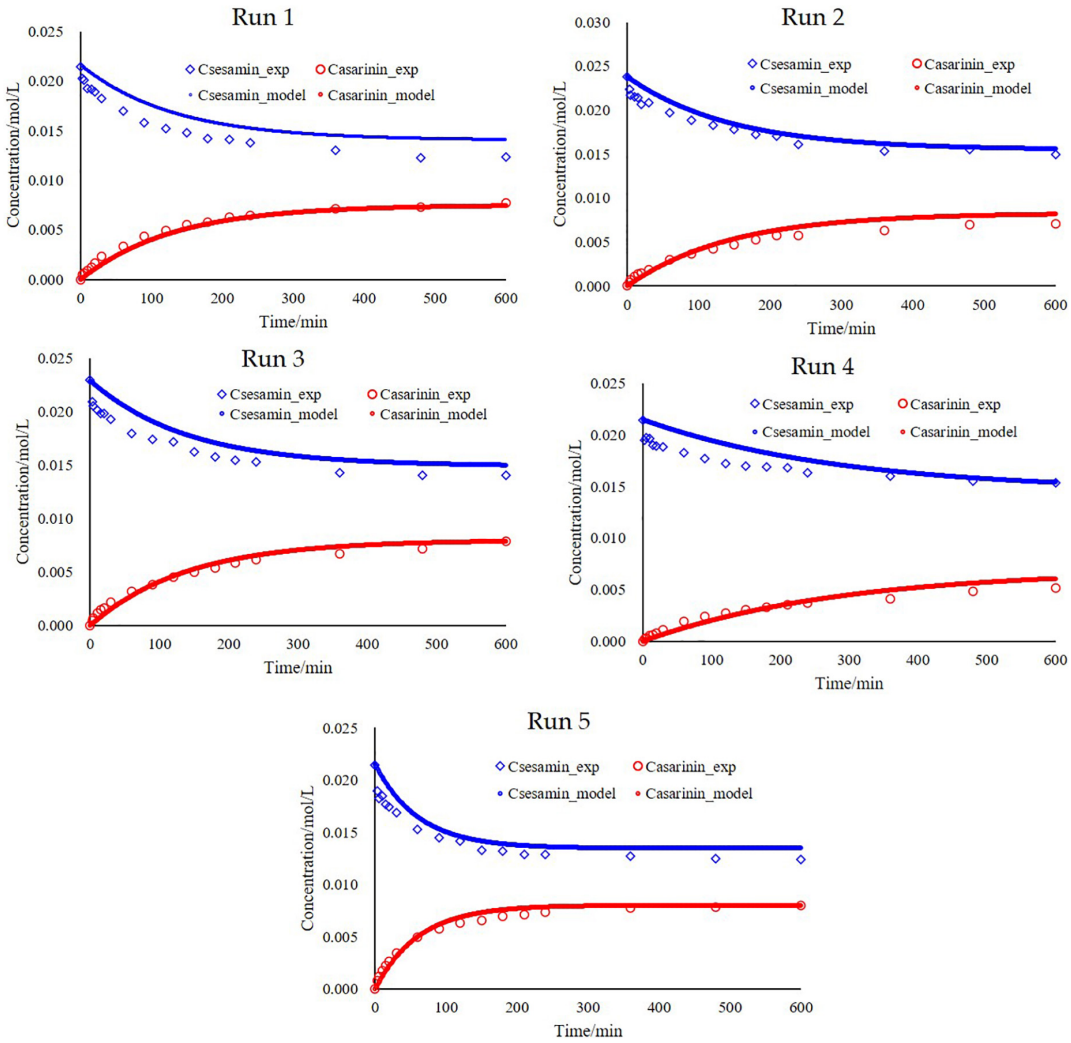

FIGURE 6
Fitting the model to the experiments and simulation of $C_{sesamin}$ and $C_{asarinin}$ for experiments 1–5. Run 1 [(C_A) = 21.47 mmol/L with catalyst loading, 1.6%; temperature, 80°C; rotation speed, 300 rpm and (C_B) = 0 mmol/L]; Run 2 [(C_A) = 23.83 mmol/L with catalyst loading, 1.6%; temperature, 80°C; rotation speed, 300 rpm and (C_B) = 0 mmol/L]; Run 3 [(C_A) = 22.91 mmol/L with catalyst loading, 1.6%; temperature, 80°C; rotation speed, 300 rpm and (C_B) = 0 mmol/L]; Run 4 [(C_A) = 21.47 mmol/L with catalyst loading, 1.6%; temperature, 70°C; rotation speed, 300 rpm and (C_B) = 0 mmol/L]; Run 5 [(C_A) = 21.47 mmol/L with catalyst loading, 1.6%; temperature, 90°C; rotation speed, 300 rpm and (C_B) = 0 mmol/L].

the material balances of the different components in this reaction system

$$\frac{d[A]}{dt} = -R_{Iso} \quad (14)$$

$$\frac{d[B]}{dt} = R_{Iso} \quad (15)$$

Modeling

To avoid correlation between the pre-exponential factor and activation energy, a modified Arrhenius equation (19, 21) was used to express the rate constants:

$$k_{Iso}(T) = exp\left[ln\left(k_{Iso,ref}\right) + \frac{E_a}{R \cdot T_{ref}} \cdot \left(1 - \frac{T_{ref}}{T}\right)\right] \quad (16)$$

where, k_{Iso} is the rate constant and E_a is activation energy (kJ/mol); the gas constant 8.314 J/(mol/K) and reaction temperature (K) are represented by R and T, respectively. In total, 353.15 K was selected as the reference temperature (T_{ref}). The equilibrium constant $K_{Iso}(T)$ can be expressed by Van't Hoof law (41, 42).

$$K_{Iso}(T) = exp\left[lnK\left(T_{ref}\right) + \frac{\triangle H_{r\ Iso}}{R \cdot T_{ref}} \cdot \left(1 - \frac{T_{ref}}{T}\right)\right] \quad (17)$$

where, T_{ref} represents the reference temperature (K) and $\triangle H_{r\ \text{Iso}}$ is the enthalpy for the sesamin conversion in kJ/mol. The kinetic constants $(ln\left(k_{\text{Iso,ref}}\right))$ and $\frac{E_a}{R\ T_{\text{ref}}}$ were estimated. Thereafter, by plotting $ln\left(\frac{K(T)}{K(T_{\text{ref}})}\right)$ versus $\left(\frac{1}{R}\left(\frac{1}{T}-\frac{1}{T_{\text{ref}}}\right)\right)$, it was demonstrated that this hypothesis is correct within the experimental temperature range. Figure 5A shows that the sesamin conversion in the sesame oil solution was endothermic ($\triangle H_{r\text{Iso}} = 34.578$ kJ/mol).

The estimated kinetic parameters for sesamin conversion and their HPD intervals are shown in Table 3. The HPD intervals for the estimated values are less than 20%, indicating that the parameter estimation for this model was accurate.

The correlation matrix for the kinetic parameters is represented in Table 4. It was observed that the correlations among different kinetic parameters are very low, indicating good reliability of the developed model.

By plotting the experimental concentrations versus the simulated values, one sees that the simulated values are close to the experimental ones with high linear correlation coefficients ($R^2_{Sesamin}$ = 0.93 and $R^2_{Asarinin}$ = 0.97), indicating that it is in good agreement with experimental data and calculated values (Figures 5B,C). Fits of the model to the experimental observations are presented in Figure 6 (Run 1–5). The kinetic model fits the experimental data well over the entire reaction, and the explanation coefficient exceeds 90%. Nevertheless, some deviations were observed (Run 1, 3, and 4). This deviation could be explained by the failure of the model to accurately take into account temperature-dependent density of the oil reaction medium and the formation of intermediate products.

Conclusion

In this study, the effects of rotation speed, reaction temperature, catalyst loading and reactant concentration on the kinetics of sesamin conversion have been investigated. The conversion of sesamin into asarinin in CSO was efficiently achieved using CA/Hβ as a catalyst. The conversion kinetics were enhanced significantly by increasing catalyst loading and reaction temperature, while the effect of rotation speed and initial concentration of reactant was found to be negligible. A kinetic model was developed to simulate the sesamin conversion process. This model was applied for a reaction temperature range of 70–90°C, catalyst loading range of 1.0–3.0%, initial reactant concentration range of 21.47–23.83 mmol/L. It was observed that the calculated data were in agreement with experimental values by parity plot ($R^2_{Sesamin}$ =0.93 and $R^2_{Asarinin}$ = 0.97), indicating the model fit the experimental data quite well. The sesamin conversion was found to be endothermic ($\triangle H_{r\ \text{Iso}} = 34.578$ kJ/mol). The CA/Hβ catalyst could be easily regenerated by calcination, and there was no obvious loss of catalytic activity when reused. In summary, this study lays the foundation for the scale-up of the production of asarinin from sesame oil using CA/Hβ as the catalyst.

Data availability statement

The original contributions presented in this study are included in the article/supplementary material, further inquiries can be directed to the corresponding author.

Author contributions

QY: investigation, data curation, and writing—original draft. X-SC: methodology, data curation, and project administration. SL: software and project administration. X-DW: funding acquisition and supervision. H-ML: supervision and project administration. C-XZ: investigation and resources. Y-XM: resources and funding acquisition. All authors contributed to the article and approved the submitted version.

Funding

This work was supported by an earmarked fund for National Natural Science Foundation of China (31972004), Doctor Research Fund of Henan University of Technology (2020BS007), and China Agriculture Research System of MOF and MARA (CARS-14).

Conflict of interest

The authors declare that the research was conducted in the absence of any commercial or financial relationships that could be construed as a potential conflict of interest.

Publisher's note

All claims expressed in this article are solely those of the authors and do not necessarily represent those of their affiliated organizations, or those of the publisher, the editors and the reviewers. Any product that may be evaluated in this article, or claim that may be made by its manufacturer, is not guaranteed or endorsed by the publisher.

References

1. Afroz M, Zihad SM, Uddin SJ, Rouf R, Rahman MS, Islam MT, et al. A systematic review on antioxidant and antiinflammatory activity of Sesame (*Sesamum indicum* L.) oil and further confirmation of anti-inflammatory activity by chemical profiling and molecular docking. *Phytother Res.* (2019) 10:2585–608. doi: 10.1002/ptr.6428

2. Jeong M, Kim HM, Lee JS, Choi JH, Jang D. (-)-Asarinin from the roots of *Asarum sieboldii* induces apoptotic cell death via caspase activation in human ovarian cancer cells. *Molecules*. (2018) 23:1849. doi: 10.3390/molecules23081849

3. Kushiro M, Masaoka T, Hageshita S, Ide T, Sugano M. Comparative effect of sesamin and episesamin on the activity and gene expression of enzymes in fatty acid oxidation and synthesis in rat liver. *J Nut Biochem.* (2002) 5:289–95. doi: 10.1016/S0955-2863(01)0024-8

4. He HP, Yang TH, Li F, Zhang LH, Ling XS. A novel study on the immunomodulatory effect of umbilical cord derived mesenchymal stem cells pretreated with traditional Chinese medicine asarinin. *Int Immunopharmacol.* (2021) 100:108054. doi: 10.1016/j.intimp.2021.108054

5. Kuo PC, Lin MC, Chen GF, Yiu TJ, Tzen JTC. Identification of methanol-soluble compounds in sesame and evaluation of antioxidant potential of its lignans. *J Agric Food Chem.* (2011) 59:3214–9. doi: 10.1021/jf104311g

6. Kim E, Kim HJ, Oh HN, Kwak AW, Kim SN, Kang BY, et al. Cytotoxic constituents from the roots of *Asarum sieboldii* in human breast cancer cells. *Nat Prod Sci.* (2019) 25:72–5. doi: 10.20307/nps.2019.25.1.72

7. Jeong SH, Jang JH, Cho HY, Lee YB. Simultaneous determination of asarinin, β-eudesmol, and wogonin in rats using ultraperformance liquid chromatography–tandem mass spectrometry and its application to pharmacokinetic studies following administration of standards and Gumiganghwal-tang. *Biomed Chromatogr.* (2021) 4:e5021. doi: 10.1002/bmc.5021

8. Li CY, Chow TJ, Wu TS. The epimerization of sesamin and asarinin. *J Nat Prod.* (2005) 68:1622–4. doi: 10.1021/np050106d

9. Chen JC, Chen YZ, Tian JJ, Ge HF, Liang XF, Xiao JB, et al. Simultaneous determination of four sesame lignans and conversion in Monascus aged vinegar using HPLC method. *Food Chem.* (2018) 256:133–9. doi: 10.1016/j.foodchem.2018.02.081

10. Tsai HY, Lee WJ, Chu IH, Hung WC, Su NW. Formation of samin diastereomers by acid-catalyzed transformation of sesamolin with hydrogen peroxide. *J Agric Food Chem.* (2020) 68:6430–8. doi: 10.1021/acs.jafc.0c01616

11. Li XD, Wang XD, Wang NN, Ma YX. Acidic catalysis and antioxidant activity of sesamolin. *Food Sci.* (2018) 39:59–64. doi: 10.7506/spkx1002-6630-201810010

12. Huang JN, Song GH, Zhang LX, Sun Q, Lu X. A novel conversion of sesamolin to sesaminol by acidic cation exchange resin. *Eur J Lipid Sci Tech.* (2012) 7:842–8. doi: 10.1002/ejlt.201100247

13. Fukuda Y, Nagata MN, Osawa T, Namiki M. Contribution of lignan analogues to antioxidative activity of refined unroasted sesame seed oil. *J Am Oil Chem Soc.* (1986) 63:1027–31.

14. Yu Q, Wang XD, Liu HM, Ma YX. Preparation and characterization of solid acid catalysts for the conversion of sesamin into asarinin in sesame oil. *Foods.* (2022) 11:1225. doi: 10.3390/foods11091225

15. Liu M, Yin YX, Guo XW, Song CS. Oxalic acid modification of β zeolite for dehydration of 2-(4'-ethylbenzoyl) benzoic acid. *Ind Eng Chem Res.* (2017) 56:8850–6. doi: 10.1021/acs.iecr.7b02235

16. Ngo H, Latona R, Sarker MI, Hums M, Moreau RA. A process to convert sunflower oil into a value added branched chain oil with unique properties. *Ind Crop Prod.* (2019) 139:111457. doi: 10.1016/j.indcrop.2019.06.020

17. Wang YY, Song H, Sun XL. Alkylation of toluene with *tert*−butyl alcohol over HPW−modified Hβ zeolite. *Chin J Catal.* (2016) 12:2134–41. doi: 10.1016/S1872-2067(16)62587-1

18. Narkhede N, Patel A. Biodiesel production by esterification of oleic acid and transesterification of soybean oil using a new solid acid catalyst comprising 12-Tungstosilicic acid and zeolite Hβ. *Ind Eng Chem Res.* (2013) 52:13637–44. doi: 10.1021/ie402230v

19. Farhoosh R. Critical kinetic parameters and rate constants representing lipid peroxidation as affected by temperature. *Food Chem.* (2021) 340:128137. doi: 10.1016/j.foodchem.2020.128137

20. Jaimez-Ordza J, Pérez-Flores JG, Castañeda-Ovando AC, González-Olivares LG, Añorve-Morga J, Contreras-López E. Kinetic parameters of lipid oxidation in third generation (3G) snacks and its influence on shelf-life. *Food Sci Tech.* (2018) 39:136–40. doi: 10.1590/fst.38917

21. Ma YQ, Wang QH, Sun XH, Wu CF, Gao Z. Kinetics studies of biodiesel production from waste cooking oil using $FeCl_3$-modified resin as heterogeneous catalyst. *Renew Energ.* (2017) 107:522–30. doi: 10.1016/j.renene.2017.02.007

22. Wang XD, Huang X, Liu S, Cui YD. Catalytic epimerization of hydrochloric acid-ferric chloride of sesamin to synthesis of asarinin and its mechanism. *CIESC J.* (2015) 66:455–60. doi: 10.11949/j.issn.0438-1157.20151447

23. Yu Q, Ma YX, Qin Z, Luo XR, Liu HM, Wang XD. Using solid acid catalysts to improve the oxidative stability of cold-pressed sesame oil. *LWT.* (2021) 141:110928. doi: 10.1016/j.lwt.2021.110928

24. Wang CY, Yen CC, Hsu MC, Wu YT. Self-nanoemulsifying drug delivery systems for enhancing solubility, permeability, and bioavailability of sesamin. *Molecules.* (2020) 25:3119. doi: 10.3390/molecules25143119

25. Shi LK, Zheng L, Jin QZ, Wang XG. Effects of adsorption on polycyclic aromatic hydrocarbon, lipid characteristic, oxidative stability and free radical scavenging capacity of sesame oil: effects of adsorption on properties of sesame oil. *Eur J Lipid Sci Tech.* (2017) 119:1700150. doi: 10.1002/ejlt.201700150

26. Tenyang N, Ponka R, Tiencheu B, Djikeng FT, Azmeera T, Karuna MSL, et al. Effects of boiling and roasting on proximate composition, lipid oxidation, fatty acid profile and mineral content of two sesame varieties commercialized and consumed in far-north region of cameroon. *Food Chem.* (2017) 221:1308–16. doi: 10.1016/j.foodchem.2016.11.025

27. Bai GY, Ma Z, Shi LJ, Lan XW, Wang YL, Han J, et al. Continuous synthesis of bis(indolyl)phenylmethane over acid modified Hβ zeolite. *Appl Catal A Gen.* (2012) 42:114–8. doi: 10.1016/j.apcata.2012.03.040

28. Yue D, Lei JH, Zhou LN, Du XD, Guo ZR, Li JS. Oxidative desulfurization of fuels at room temperature using ordered meso/macroporous $H_3PW_{12}O_{40}/SiO_2$ catalyst with high specific surface areas. *Arab J Chem.* (2020) 13:2649–58. doi: 10.1016/j.arabjc.2018.06.017

29. Stewart WE, Caracotsios M. *Computer-Aided Modeling of Reactive Systems*. Hoboken, NJ: Wiley (2008). doi: 10.1002/9780470282038

30. Capecci S, Wang YJ, Moreno VS, Held C, Leveneur S. Solvent effect on the kinetics of the hydrogenation of *n*-butyl levulinate to γ-valerolactone. *Chem Eng Sci.* (2021) 231:116315. doi: 10.1016/j.ces.2020.116315

31. Caracotsios M, Stewart WE. Sensitivity analysis of initial value problems with mixed ODEs and algebraic equations. *Comput Chem Eng.* (1984) 9:359–65.

32. Cai XS, Tolvanen P, Virtanen P, Eränen K, Rahkila J, Leveneur S, et al. Kinetic study of the carbonation of epoxidized fatty acid methyl ester catalyzed over heterogeneous catalyst HBimCl-$NbCl_5$/HCMC. *Int J Chem Kinet.* (2021) 53:1203–19. doi: 10.1002/kin.21526

33. Ji JM, Xie WL. Removal of aflatoxin B_1 from contaminated peanut oils using magnetic attapulgite. *Food Chem.* (2021) 339:128072. doi: 10.1016/j.foodchem.2020.128072

34. Guechi EK, Hamdaoui O. Sorption of malachite green from aqueous solution by potato peel: kinetics and equilibrium modeling using non-linear analysis method. *Arab J Chem.* (2016) 9:S416–24. doi: 10.1016/j.arabjc.2011.05.011

35. Satyarthi JK, Radhakrishnan S, Srinivas D. Factors influencing the kinetics of esterification of fatty acids over solid acid catalysts. *Energ Fuel.* (2011) 25:4106–12. doi: 10.1021/ef2009138

36. Kuniyil M, Kumar JVS, Adil SF, Assal ME, Shaik MR, Khan M, et al. Production of biodiesel from waste cooking oil using ZnCuO/N-doped graphene nanocomposite as an efficient heterogeneous catalyst. *Arab J Chem.* (2021) 14:102982. doi: 10.1016/j.arabjc.2020.102982

37. Yusuff AS, Bhonsle AK, Bangwal DP, Atray N. Development of a barium-modified zeolite catalyst for biodiesel production from waste frying oil: process optimization by design of experiment. *Renew Energ.* (2021) 177:1253–64. doi: 10.1016/j.renene.2021.06.039

38. Bukhtiyarova MV, Toktare AV, Kazakov MO, Kodenev EG, Pereyma VY, Gabrienko AA, et al. Effect of sulfosalicylic acid treatment on the properties of Beta zeolite and performance of NiW/Beta-based catalysts in hexadecane hydrocracking. *Appl Catal A Gen.* (2020) 598:117573. doi: 10.1016/j.apcata.2020.117573

39. Aguilera AF, Tolvanen P, Eränen K, Wärna J, Leveneur S, Marchant T, et al. Kinetic modelling of Prileschajew epoxidation of oleic acid under conventional heating and microwave irradiation. *Chem Eng Sci.* (2019) 199:426–38. doi: 10.1016/j.ces.2019.01.035

40. Agudelo AFG, Pérez-Sena WY, Kebir N, Salmi T, Ríos LA, Leveneur S. Influence of steric effects on the kinetics of cyclic-carbonate vegetable oils aminolysis. *Chem Eng Sci.* (2020) 228:115954. doi: 10.1016/j.ces.2020.115954

41. Cai XS, Zheng JL, Aguilera AF, Vernières-Hassimi L, Tolvanen P, Salmi T, et al. Influence of ring-opening reactions on the kinetics of cottonseed oil epoxidation. *Int J Chem Kinet.* (2018) 50:726–41. doi: 10.1002/kin.21208

42. Russo V, Tesser R, Rossano C, Cogliano T, Vitiello R, Leveneur S, et al. Kinetic study of Amberlite IR_{120} catalyzed acid esterification of levulinic acid with ethanol: from batch to continuous operation. *Chem Eng J.* (2020) 401:126126. doi: 10.1016/j.cej.2020.126126